Journal of Power Sources 225 (2013) 179–186

Contents lists available at SciVerse ScienceDirect

Journal of Power Sources

journal homepage: www.elsevier.com/locate/jpowsour

Effective diffusivity of gas diffusion layer in proton exchange membrane fuel cells

Dahua Shou [a,b,*], Jintu Fan [a,c,**], Feng Ding [a]

[a] Institute of Textiles and Clothing, The Hong Kong Polytechnic University, Hung Hom, Kowloon, Hong Kong
[b] Centre for Advanced Materials Technology (CAMT), School of Aerospace, Mechanical and Mechatronic Engineering, The University of Sydney, NSW 2006, Australia
[c] Department of Fiber Science & Apparel Design, College of Human Ecology, Cornell University, Ithaca, NY, USA

HIGHLIGHTS

- We develop a comprehensive diffusivity model for gas diffusion layers (GDLs) in proton exchange membrane fuel cells (PEMFCs).
- The analytical model agrees excellently with experimental results and numerical data available in literature.
- The influences of microstructures of GDLs are extensively explored.

ARTICLE INFO

Article history:
Received 4 August 2012
Received in revised form
5 October 2012
Accepted 12 October 2012
Available online 23 October 2012

Keywords:
Effective diffusivity
Analytical model
Fibrous media
Proton exchange membrane fuel cell
Gas diffusion layers

ABSTRACT

In gas diffusion layers (GDLs) of proton exchange membrane fuel cells (PEMFCs), effective gas diffusivity is a key parameter to be determined and engineered. Existing theoretical models of effective diffusivity are limited to one-dimensional (1D) regular fiber arrays. Numerical simulations were carried out to simulate gas diffusion through more realistic fibrous materials like GDLs, in which fibers are randomly distributed in a two-dimensional (2D) plane or three-dimensional (3D) space, but they could not fully reveal the underlying mechanisms. In this paper, we propose an analytical model to predict the effective diffusivities of 1D, 2D and 3D randomly distributed fiber assembles. The present model is established by extending the model of 1D regular fiber alignments to 1D random fiber arrangements through Voronoi Tessellation method, and using the 1D local diffusivities to determine the 2D and 3D diffusivities based on mixing rules. The predicted effective diffusivities agree well with experimental results and numerical data. With the new model, the influences of porosity, fiber distribution, and fiber orientation are analyzed in this study.

1. Introduction

Proton exchange membrane fuel cell (PEMFC) is considered to be one of the leading candidates for the power sources of mobile, stationary, and portable devices [1]. The gas diffusion layer (GDL) of PEMFCs is a fibrous porous material with a layered structure, which not only provides the support of the fuel cell membrane, but also allows the transport of reactant products. For example, oxygen diffuses through the GDL from the gas channel (GC) to the catalyst layer (CL), where it is combined with the protons and electrons from the anode to produce water [2]. The produced water could condense and even block the porous GDL. Therefore, effective diffusivities of water vapor, oxygen, and hydrogen strongly affect the PEMFC's performance.

The movement of gas molecules caused by concentration difference in a porous medium is known as diffusion [3]. It takes place when the concentration of the molecules is higher in one region than the other. Gas molecules will not stop migrating until there is an equalized concentration configuration throughout the carrier. The moving paths of molecules during diffusive motion process are random, but the most preferred migration of molecules will be in the direction of decreasing concentration. Generally, gas diffusion through a medium can be phenomenologically described by Fick's law:

$$J = D_{\text{eff}} \nabla C, \tag{1}$$

where, J is the diffusive flux, D_{eff} is the effective diffusivity and ∇C is the concentration gradient. Fick's law states that the average flux in the fibrous structure is directly proportional to the gas

* Corresponding author. Institute of Textiles and Clothing, The Hong Kong Polytechnic University, Hung Hom, Kowloon, Hong Kong. Tel.: +852 2766 6472; fax: +852 2773 1432.
** Corresponding author. Department of Fiber Science & Apparel Design, College of Human Ecology, Cornell University, Ithaca, NY, USA.
E-mail addresses: dhshou@gmail.com (D. Shou), jf456@cornell.edu (J. Fan).

0378-7753/$ – see front matter © 2012 Elsevier B.V. All rights reserved.
http://dx.doi.org/10.1016/j.jpowsour.2012.10.039

concentration gradient, and the effective diffusivity tensor D_{eff} lumps all the complex interactions between gas and fiber. Accurate determination of effective diffusivity, therefore, is essential to characterize the diffusion process.

The effective diffusivity of fibrous materials can be determined through Eq. (1) by experimentally measuring the diffusive flux and the directional concentration gradient. Early in 1940, through-plane diffusion coefficient of a steel wool sample was measured using carbon disulfide and acetone vapor [4]. In 1984, Bateman et al. [5] employed NO gas to transfer through a 2D cellulosic filter and calculated its effective diffusivity. Recently, Gibson et al. [6] applied a dynamic diffusion test cell method to measure vapor diffusivity of fibrous media. Two parallel gas flows with different water vapor humidity were directed to a test cell, with which vapor diffused through the sample between the gas flows, and the effective diffusivity was determined by measuring the relative humidity of gas flows leaving the cell [6]. Huang and Qian [7] modified the dynamic cell method by providing a water vapor source on one side of the sample. Effective diffusivities of GDLs were also obtained indirectly by measuring ionic conductivity for the soaped electrolyte based on the analogy between Ohm's law and Fick's law [8–10]. Using a dynamic diffusion cell, LaManna and Kandlikar [11] recently investigated the effects of Microporous Layer (MPL) coatings, GDL thickness, and polytetrafluorethylene (PTFE) loadings on the effective water vapor diffusion coefficient of GDLs. Instead of measuring the effective diffusivity, many measured the evaporative moisture vapor resistance, which is inversely related to the vapor diffusivity [12,13].

Many researchers modeled the gas diffusion through fibrous materials. The simplest model assumes the fibrous material consisting of a bundle of tortuous channels. So the effective diffusivity is related to the bulk diffusivity in the void through porosity and tortuosity, given by a normalized form [14], viz:

$$\frac{D_{eff}}{D_b} = \frac{\varepsilon}{\tau}, \tag{2}$$

where D_b is the gas diffusivity in the void, ε is the porosity, and τ is the tortuosity. Although porosity is easy to be calculated or measured, the applicability of Equation (2) is tarnished by the difficulty in accurately determining the value of tortuosity [15]. A pore-scale model was presented to predict the effective diffusivity of unconsolidated porous media based on a rectangular representative unit cell, in which the tortuosity was expressed as the ratio of the diffusive path length to the streamwise displacement [16]. However, the regular geometry of the diffusive streamlines in the pore-scale model is over-idealized.

Apart from the pore-based models above, fiber-based models were developed. Shen and Springer [17] calculated diffusive transport across 1D impermeable cylinders with square packing configuration in a rectangular unit cell, and the model of effective diffusivity was expressed as:

$$\frac{D_{eff}}{D_b} = 1 - 2\sqrt{\frac{1-\varepsilon}{\pi}}, \tag{3}$$

which was widely applied to evaluate the influence of water vapor diffusion on the mechanical properties of composites [18]. Nevertheless, this model did not consider the varying width of the gaps between cylindrical fibers and hence under-estimates the effective diffusivity. The varying width of the gap between cylindrical fibers was later considered by Li et al. [19] for both square and hexagonal fibers arrangement, but their model over-predicts the diffusivity as the gas concentration is assumed to be constant at any cross-section in the channel between the fibers. In the PEMFC literature, the Bruggeman model has attracted most of the attention [20]. The Bruggeman model is based on effective medium approximation and is given by:

$$\frac{D_{eff}}{D_b} = \varepsilon^{1.5}. \tag{4}$$

However, the Bruggeman model was derived for uniformly packed spherical particles rather than differently oriented cylindrical fibers.

In order to model gas diffusion through more realistic fibrous structures, a number of researchers applied a variety of numerical simulation techniques. Tomadakis and Sotirchos [14] performed Monte Carlo simulations for 1D, 2D and 3D randomly oriented fibers and calculated the effective diffusivity. They measured the mean traveling distances of diffusive molecules inside the numerical fiber network, and proposed the following model for the randomly oriented fibrous systems:

$$\frac{D_{eff}}{D_b} = \varepsilon\left(\frac{\varepsilon-\varepsilon_p}{1-\varepsilon_p}\right)^{\beta}, \tag{5}$$

where, ε_p is the percolation threshold and β is an empirical constant determined by a least squares fit to the simulation results. In another numerical study, the local effective diffusivity of a GDL medium was determined as a function of the local porosity and the local water saturation by a network model, where the solid structure was simulated as layers of fiber screens and each layer was shifted by a randomly selected in-plane distance [21]. In 2008, Becker et al. [22] numerically reconstructed a fibrous structure from a 3D tomography image of the GDL, and proposed the effective diffusivity as a function of the saturation of the GDL. Later in 2011, Becker et al. [23] extended their work to consider the effect of Microporous Layer (MPL).

Although many analytical models have been proposed for determining the effective diffusivity of fibrous materials, they are limited to 1D fiber arrays. For more realistic fibrous materials where fibers are 2D or 3D oriented, only numerical studies have been conducted, which cannot fully reveal the underlying mechanisms of gas diffusion. In this work, we propose a generalized analytical model of effective diffusivity of fibrous materials. The new model is established through first extending the model of regular 1D fiber arrays to random 1D fiber arrays by Voronoi Tessellation approximation, and then applying them to 2D and 3D random fiber assembles by mixing rules.

2. Model generation

In this paper, fibrous media are assumed to be composed of periodical unit cells representing the geometrical nature of the microstructures. The present model is established by extending the model for regular 1D fiber arrays, since although the architectures of fibrous media vary from simple 1D regular type to complex 2D and 3D cases, they can be approximately represented by mixtures of 1D fibers arrays [24,25]. The following assumptions are made:

1. The fibrous matrix is made up of straight and circular fibers with relatively high porosity.
2. All the fibers are impermeable and the gas diffusion takes place only in the void areas between fibers.
3. The fibrous media have relatively high porosity and the spacing between fibers is much larger than the mean free path of diffusing species.

The simplest representative cell for 1D fibrous media is regular array of parallel fibers as shown in Fig. 1. The diffusivity in the open

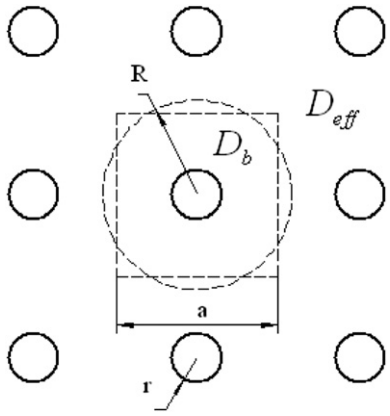

Fig. 1. A unit cell in regular array of parallel fibers. The square has the same area with the circle in dotted line.

voids of the cell is equal to bulk diffusivity D_b, which characterizes gas diffusion in bulk space without confinement. This representative cell is composed of an impermeable fiber and the gas matrix, surrounded by the effective medium with diffusivity D_{eff}, which is the same as the diffusivity of the whole system. For convenience and without losing generality, the representative cell is assumed to be a circle with the same area of the square containing the fiber. The porosity ε for this arrangement of, both the unit cell and the whole fibrous system can be determined by the following equation:

$$\varepsilon = 1 - \frac{\pi r^2}{a^2} = 1 - \frac{r^2}{R^2}, \tag{6}$$

where r is the fiber radius, R is the radius of the unit cell, a is the edge length of the square. In a steady state, the gas diffusion across the fiber array is defined by the following Laplace equation [26]:

$$\nabla^2 C(l,\theta) = 0, \tag{7}$$

where l and θ are the cylindrical coordinates. The appropriate solution of Eq. (7) for diffusion normal to fibers reads [27]:

$$C(l,\theta) = \begin{cases} Al\cos\theta, & (0 < l \le r) \\ \left(Bl + \dfrac{E}{l}\right)\cos\theta, & (r < l \le R), \\ Gl\cos\theta, & (R < l) \end{cases} \tag{8}$$

where A, B, E, and G are unknown constants arising from boundary conditions.

The continuity of the diffusive gas at the boundary between the impermeable fiber and the gas leads to:

$$Br + \frac{E}{r} = Ar = 0, \tag{9}$$

and there is no gas diffusion flux passing through the boundary of fiber surface:

$$D_b\left(B - \frac{E}{r^2}\right) = 0. \tag{10}$$

The continuity of the diffusive gas at the boundary of the unit cell results in:

$$BR + \frac{E}{R} = GR, \tag{11}$$

and the gas diffusion rate is equal for both at the boundary of the unit cell:

$$D_b\left(B - \frac{E}{R^2}\right) = D_{eff}G. \tag{12}$$

Solving the equations of (9)–(12), the through-plane effective diffusivity (i.e. gas diffusion normal to fiber arrays or layers) for both the unit cell and the whole 1D regular fibrous system is obtained:

$$\frac{D_{eff}}{D_b} = \frac{R^2 - r^2}{R^2 + r^2}, \tag{13}$$

or in forms of porosity ε:

$$\frac{D_{eff}}{D_b} = \frac{\varepsilon}{2 - \varepsilon}. \tag{14}$$

Then we consider the more complicated and realistic structures, in which fibers are placed randomly. Diffusion process through the fibrous system becomes more complex because of the disorder of the fiber arrangement. In the fibrous system composed of randomly located fibers, one fiber is assumed to be contained by a polygonal cell whose boundaries are defined by the perpendicular bisectors of the lines joining each fiber with its nearest neighbor, as presented in Fig. 2. The polygonal cell is called Voronoi Tessellation [28], which is used to characterize the randomness of fiber distribution in this study.

It is reasonable to assume that the highly porous fibrous system is homogeneous macroscopically with a constant concentration gradient, but different diffusion coefficients in each cell. Thus, the effective diffusive flux J_{eff} of the system can be obtained in a volume-averaged form:

$$J_{eff} = \frac{\int J\mathrm{d}S}{\int \mathrm{d}S} = \frac{\sum J(\Delta S)\Delta S}{\sum \Delta S} = \frac{\sum_{i=0}^{N} J(S_i)S_i}{\sum_{i=0}^{N} S_i}, \tag{15}$$

where $J(S_i)$ and S_i are the flux and area of the ith unit cell, respectively, N is the number of the unit cells in the system, and $\langle S\rangle$ is the mean area of the unit cells. As N is very large and S_i is very small comparing with the crossing area of the whole system, the effective diffusive flux J_{eff} can be expressed as a function of probability density of unit cell area $f(S)$ in an integral form:

$$J_{eff} = \int J(S)f(S)\mathrm{d}S. \tag{16}$$

Substituting Eq. (16) into Eq. (1) leads to the effective diffusivity:

$$D_{eff} = \int D(S)f(S)\mathrm{d}S. \tag{17}$$

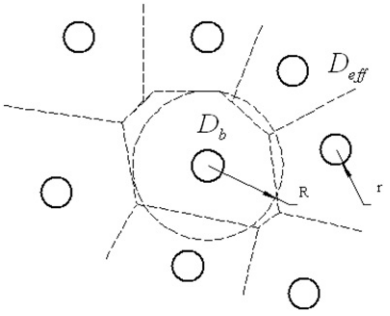

Fig. 2. A unit cell in randomly distributed array of parallel fibers. The voronoi has the same area with the circle in dotted line.

The local cell area distribution in the Voronoi Tessellation is well described by the Gamma distribution [29]:

$$f(S) = \frac{\alpha^\alpha}{\langle S\rangle^\alpha}\frac{S^{\alpha-1}}{\Gamma(\alpha)}e^{-\alpha\frac{S}{\langle S\rangle}}, \tag{18}$$

where $\Gamma(\alpha)$ is a Gamma distribution, and α is the scale parameter.

It satisfies the following equations:

$$\int_{\pi r^2}^{\infty} f(S)\mathrm{d}S = 1, \tag{19}$$

and

$$\int_{\pi r^2}^{\infty} Sf(S)\mathrm{d}S = \langle S\rangle. \tag{20}$$

In analogous to the assumption successfully applied to the study of more structure-sensitive gas flow [24], this model assumes that the diffusivity within the voronoi is identical to that within the circle of the same area as shown in Fig. 2. Substituting Eq. (13) and Eq. (18) into Eq. (17), the normalized through-plane effective diffusivity of 1D random fibrous media is derived:

$$\frac{D_{\mathrm{eff}}}{D_{\mathrm{b}}} = \int_{\pi r^2}^{\infty} \frac{S-\pi r^2}{S+\pi r^2}\frac{\alpha^\alpha}{\Gamma(\alpha)}\left(\frac{S}{\langle S\rangle}\right)^{\alpha-1}e^{-\alpha\frac{S}{\langle S\rangle}}\mathrm{d}\left(\frac{S}{\langle S\rangle}\right). \tag{21}$$

Re-writing Eq. (21) with $\varepsilon = 1-(\pi r^2/\langle S\rangle)$ and $x = S/\langle S\rangle$, we can obtain the following equation of normalized through-plane diffusivity:

$$\frac{D_{\mathrm{eff}}}{D_{\mathrm{b}}} = \int_{1-\varepsilon}^{\infty} \frac{\alpha^\alpha}{\Gamma(\alpha)}\frac{x-1+\varepsilon}{x+1-\varepsilon}x^{\alpha-1}e^{-\alpha x}\mathrm{d}x. \tag{22}$$

The scale parameter α is numerically determined by Monte Carlo Simulation. For randomly distributed fibers, $\alpha = 3.5$ [30] and Eq. (22) becomes:

$$\frac{D_{\mathrm{eff}}}{D_{\mathrm{b}}} = 24\int_{1-\varepsilon}^{\infty} \frac{x-1+\varepsilon}{x+1-\varepsilon}x^{2.5}e^{-3.5x}\mathrm{d}x. \tag{23}$$

For gas diffusion parallel with fibers, the tortuosity of the 1D fibrous medium is found to be almost independent of its porosity, and the in-plane effective diffusivity (i.e. gas diffusion parallel with fiber arrays or layers) for both regular and random 1D fibers is given by [31]:

$$\frac{D_{\mathrm{eff}}}{D_{\mathrm{b}}} = \varepsilon. \tag{24}$$

The model for 1D random fibers described by Equation (23) also applies to 2D random fibrous structures, since the through-plane effective diffusivity is not sensitive to in-plane fiber orientation. This was demonstrated from the past numerical simulation [14] and can also be inferred from the fact that gas diffusion is less affected by the presence of fibers than the pressure-driven gas flow, and the gas permeability was shown to be independent of in-plane fiber orientation [32,33].

For 3D fibrous materials with some fibers more aligned with the principal direction of gas diffusion, the exact solution of gas diffusivity is difficult to obtain. In this study, the effective diffusivity is estimated from a combination of local diffusivities of 1D fiber arrays normal to and that of 1D fiber arrays parallel with the diffusion direction (see Fig. 3). Although the distribution of fibers in a 3D fibrous material is complex, it can be considered that the entire 3D fibrous system is homogeneous at macro-scale and the average porosity of the fraction of the fibers oriented in the three principle directions (x-, y- or z-direction) shares the same average porosity of the whole fibrous system. Three mixing rules, which were proposed for permeability prediction [25], are also used in this study to determine effective diffusivities based on the mathematical analogy between Darcy's law and Fick's law. The three mixing rules based on different approximations and as functions of fiber fraction $\varphi = 1-\varepsilon$ are listed as follows:

$$D_{\mathrm{eff}}(\phi) = \frac{\phi_{\mathrm{norm}}}{\phi}D_{\mathrm{norm}}(\phi) + \frac{\phi_{\mathrm{par}}}{\phi}D_{\mathrm{par}}(\phi), \tag{25}$$

$$D_{\mathrm{eff}}(\phi) = \left[\frac{\phi_{\mathrm{norm}}}{\phi}D^{-1}_{\mathrm{norm}}(\phi) + \frac{\phi_{\mathrm{par}}}{\phi}D^{-1}_{\mathrm{par}}(\phi)\right]^{-1}, \tag{26}$$

$$D_{\mathrm{eff}}(\phi) = [D_{\mathrm{norm}}(\phi)]^{\frac{\phi_{\mathrm{norm}}}{\phi}}[D_{\mathrm{par}}(\phi)]^{\frac{\phi_{\mathrm{par}}}{\phi}}, \tag{27}$$

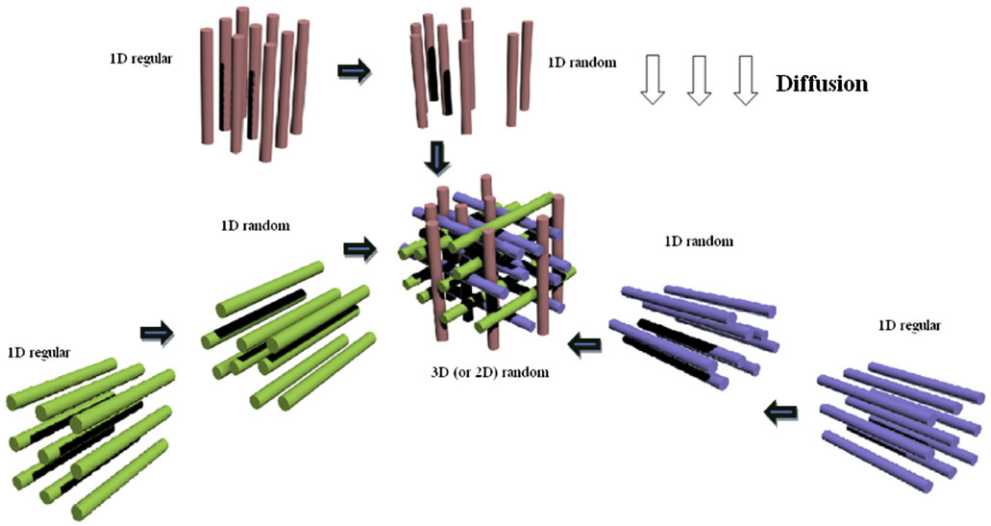

Fig. 3. Illustration of 3D or 2D fibrous media composed of 1D fiber arrays.

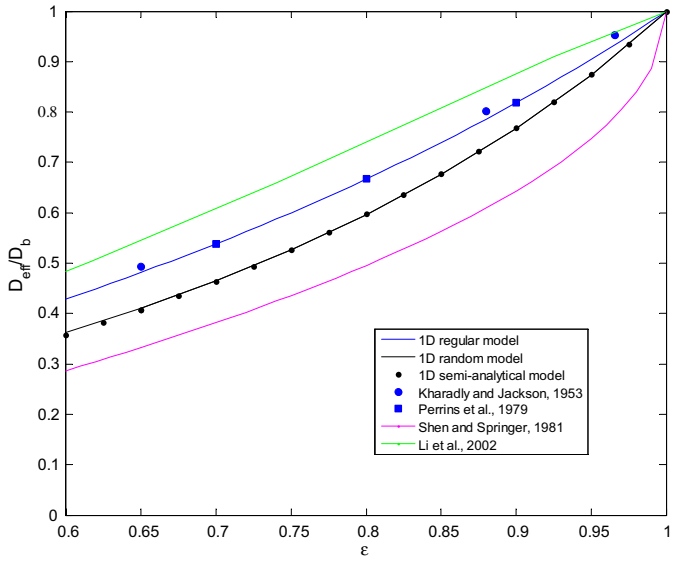

Fig. 4. Comparison of the model of 1D through-plane diffusivity with experimental, numerical, and analytical results.

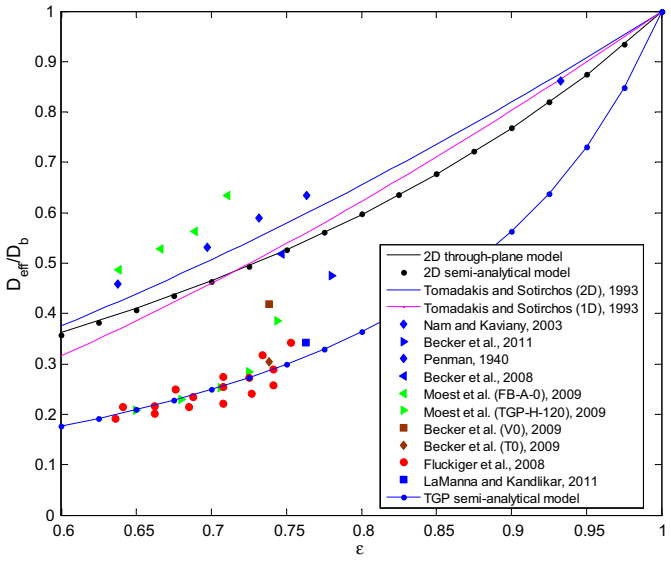

Fig. 6. Comparison of the model of 2D through-plane diffusivity with experimental and numerical results.

where, "norm" and "par" mean normal to and parallel with the diffusion direction, respectively. In Eq. (25), the volume-weighted diffusivity assumes fibers parallel to the diffusion direction and fibers normal to the diffusion direction as parallel resistors. In Eq. (26), fibers parallel to the diffusion direction and fibers normal to the diffusion direction are considered in series. Eq. (27) gives a geometric mean by a mathematical blend without physical meaning.

3. Model validation and discussions

Prediction of the proposed model is compared with numerical, experimental and analytical results available in the literature. Since the data in the literature were reported in terms of tortuosity, equivalent diffusivity, diffusive resistance, or other related parameters, they were first converted to normalized effective diffusivity for direct comparison with the prediction of the present model. For the purpose of this comparison, we assume $\phi_{norm} = \phi_{para} = 1/2$ for in-plane gas diffusion of 2D fibrous media; and we assume $\phi_{norm} = 2/3$, and $\phi_{para} = 1/3$ for through-plane gas diffusion of 3D fibrous media.

The normalized through-plane effective diffusivities calculated for 1D fiber arrays in regular and random packing are plotted in Fig. 4. For 1D fiber arrays in regular packing, the results of the present model match almost perfectly with the numerical results of Perrins et al. [34] and the experimental data from Kharadly and Jackson [35]. However, the results of our model are considerably different from those of Shen and Springer's model [17], who did not consider the width variation of the void channel between fibers. The prediction of Li et al. [19] is a little higher than that of the present model, which may arise from their over-idealized assumption that gas concentration is uniform at any cross-section of the void channel.

Substituting Eq. (14) into Eq. (2), we can get the tortuosity of 1D fiber arrays with regular packing when the fibers are normal to gas diffusion:

$$\tau = 2 - \varepsilon. \tag{28}$$

Based on the widely used equation for tortuosity of porous media [36], $\tau = 1 + 0.8(1 - \varepsilon)$, a more general form of tortuosity correlation is obtained as follows [15]:

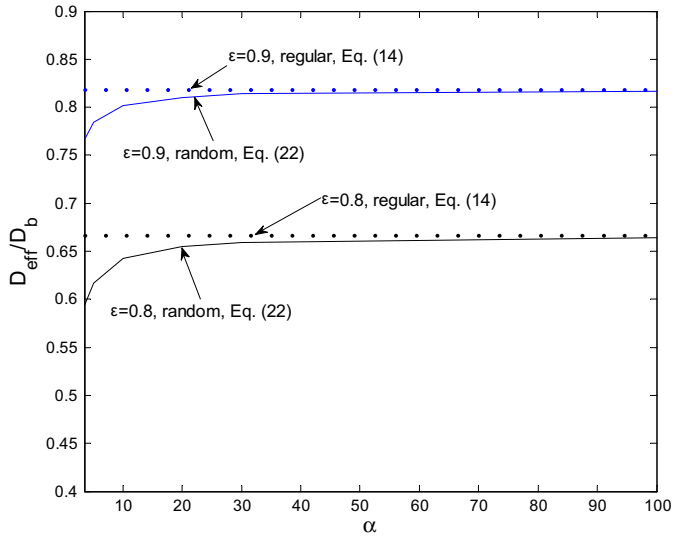

Fig. 5. Normalized effective diffusivity of 1D fiber arrays as a function of randomness measure α at $\varepsilon = 0.8$ and $\varepsilon = 0.9$.

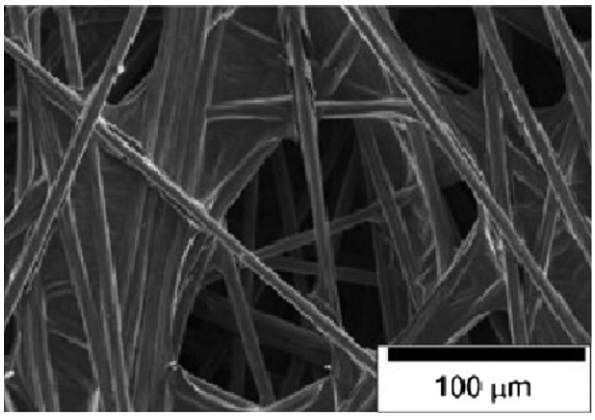

Fig. 7. SEM image of TGP-060 GDL substrate with binder [9].

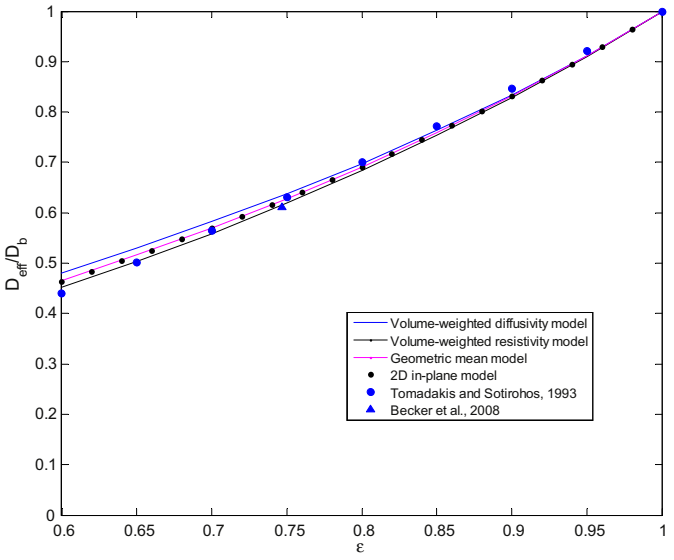

Fig. 8. Comparison of the mixing laws of 2D in-plane diffusivity with numerical results.

$$\tau = 1 + k(1-\varepsilon), \tag{29}$$

where k is an empirical constant. In this study, Eq. (29) is employed to determine the tortuosity of fibrous media, and a semi-analytical model of effective diffusivity is obtained based on Eqs. (2) and (29), viz.

$$\frac{D_{\text{eff}}}{D_{\text{b}}} = \frac{\varepsilon}{1 + k(1-\varepsilon)}. \tag{30}$$

Apparently, Eq. (30) can be deduced to Eq. (14) for 1D regular fibers when $k = 1$. In addition, it can be seen in Fig. 4 that Eq. (30) matches excellently with the 1D random model of Eq. (23) by adjusting the constant $k = 1.7$. Therefore, the semi-analytical model of 1D randomly located fibers is given by:

$$\frac{D_{\text{eff}}}{D_{\text{b}}} = \frac{\varepsilon}{2.7 - 1.7\varepsilon}. \tag{31}$$

Fig. 4 also shows that the through-plane effective diffusivity of 1D random structure is slightly lower than that of 1D regular structure, which can be explained by the fact that more random and disordered structures lead to longer tortuous paths for diffusive molecules. When the scale parameter α in Eq. (22) increases, the cell areas of fiber alignments in Fig. 2 become more uniformly distributed. The 1D through-plane diffusivity from Eq. (22) tends to be equal to that from Eq. (14) when α is very large, as seen in Fig. 5. It is interesting to note that the effect of randomness on viscous gas flow though fibrous media is different from the effect of randomness on gas diffusion. The gas permeability of fibrous media increases with increasing randomness [37], but the gas diffusivity reduces with increasing randomness of fiber arrangements. Therefore, when fibers are less randomly located, the fibrous structures will have lower gas flow permeability but higher gas diffusivity, making them better candidates of breathable materials.

In order to validate the present model, past numerical and experimental results of GDLs are plotted and compared with the prediction of the present model in Fig. 6. Tomadakis and Sotirchos [14] investigated the diffusivities through 1D and 2D randomly located fiber assembles using Monte Carlo simulation and found that 1D and 2D through-plane diffusivities are similar. As can be seen from Fig. 6, both 1D and 2D through-plane diffusivities from Tomadakis and Sotirchos [14] are close to our 2D (1D) through-plane model of Eq. (23), which shows that 1D and 2D through-plane diffusivities are approximately independent of in-plane fiber orientation. We can also see from the figure that our model prediction agrees well with the experimental data from Penman [4] and Moest et al. [10] and the numerical simulation results by Nam and Kaviany [21] and by Becker et al. [22,23]. Nevertheless, it should be noted that our model prediction deviates greatly from some experimental data in the literature [9–11]. This is due to the fact that chemical binders were applied in the samples of these experiments, but not considered in our model. The binder used to bind carbon fibers together can fill the voids between the fibers (see Fig. 7 from Ref. [9]). Therefore, the effective diffusivities measured in these experiments (e.g. the experimental results of Toray TGP-060 carbon fibers by Flueckiger et al. [9] and Toray TGP-120 carbon fibers by Moest et al. [10] and LaManna and Kandlikar [11]) are significantly lower than the model prediction. Moest et al. [10] also measured effective diffusivity of Freudenberg FB-A-0 carbon fiber layers, which are bonded mechanically without chemical binder, and the experimental data were comparable with the present model of 2D through-plane diffusivity. In addition, numerical simulations by Becker et al. [38] show that the virtually created GDL with binder converged on the fiber contacting area (V0) had higher diffusivity than the reconstructed GDL based on the tomographic image of real TGP-060 paper (T0), as seen in Fig. 6. Therefore, high performance of PEMFCs with improved gas diffusivity can be achieved with less binder used or less binder distributed in void pores between fibers. We also provide a semi-analytical model fitted by the diffusivities of TGP carbon fibers [9–11] based on Eq. (30):

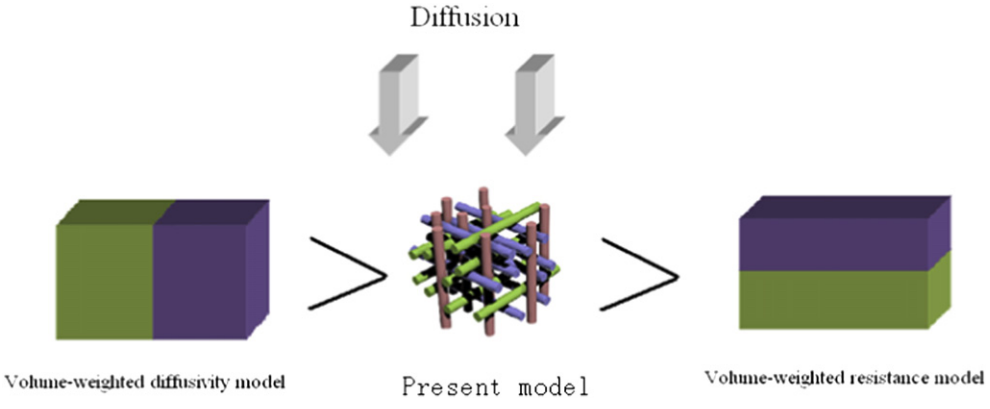

Fig. 9. Relationship between the realistic model, volume-averaged diffusivity model, and volume-averaged resistance model.

$$\frac{D_{\text{eff}}}{D_{\text{b}}} = \frac{\varepsilon}{7-6\varepsilon}. \tag{32}$$

In Fig. 8, the 2D in-plane diffusivity of a fibrous material, consisting of 1D random fibers, assuming half fibers parallel and half normal to flux direction, predicted by the present model using three different mixing rules, is compared with the numerical results from Tomadakis and Sotirchos [14] and Becker et al. [22]. It is interesting to see that there is only very small difference between the results based on the three mixing rules, and the model prediction using either of the mixing rules agree well with the numerical results. The volume-averaged diffusivity model and the volume-averaged resistance model are the upper and lower limits of diffusivity estimates, respectively (see Fig. 9), while the geometric mean is merely a mathematical estimate without physical meaning. Therefore, a better estimate would be the average of volume-averaged diffusivity model and volume-averaged resistance model, which is adopted in this study and plotted in Fig. 8:

$$\begin{aligned} D_{\text{eff}}(\phi) =& \frac{1}{2}\left[\frac{\phi_{\text{norm}}}{\phi}D_{\text{norm}}(\phi) + \frac{\phi_{\text{par}}}{\phi}D_{\text{par}}(\phi)\right] \\ &+ \frac{1}{2}\left[\frac{\phi_{\text{norm}}}{\phi}D^{-1}_{\text{norm}}(\phi) + \frac{\phi_{\text{par}}}{\phi}D^{-1}_{\text{par}}(\phi)\right]^{-1}. \end{aligned} \tag{33}$$

Based on Eqs. (24), (31) and (33), the 2D in-plane diffusivity model can be expressed as:

$$\frac{D_{\text{eff}}}{D_{\text{b}}} = \frac{\varepsilon}{4}\left(\frac{3.7-1.7\varepsilon}{2.7-1.7\varepsilon} + \frac{4}{3.7-1.7\varepsilon}\right). \tag{34}$$

Likewise, comparison of three different mixing rules is carried out for 3D through-plane diffusivity in Fig. 10. The prediction of our model for the 3D fibrous structure, assuming it consists of 1D random fibers with 1/3 parallel with and 2/3 normal to diffusion direction, agrees well with the numerical data by Tomadakis and Sotirchos [14]. Based on Eqs. (24), (31) and (33), we can derive a semi-analytical model for 3D fibrous structure:

$$\frac{D_{\text{eff}}}{D_{\text{b}}} = \frac{\varepsilon}{6}\left(\frac{4.7-1.7\varepsilon}{2.7-1.7\varepsilon} + \frac{9}{6.4-3.4\varepsilon}\right). \tag{35}$$

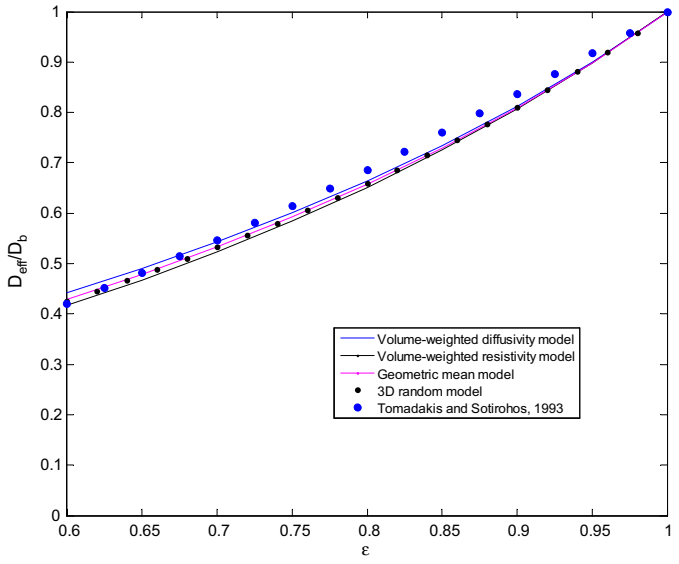

Fig. 10. Comparison of the mixing laws of 3D through-plane diffusivity with numerical results.

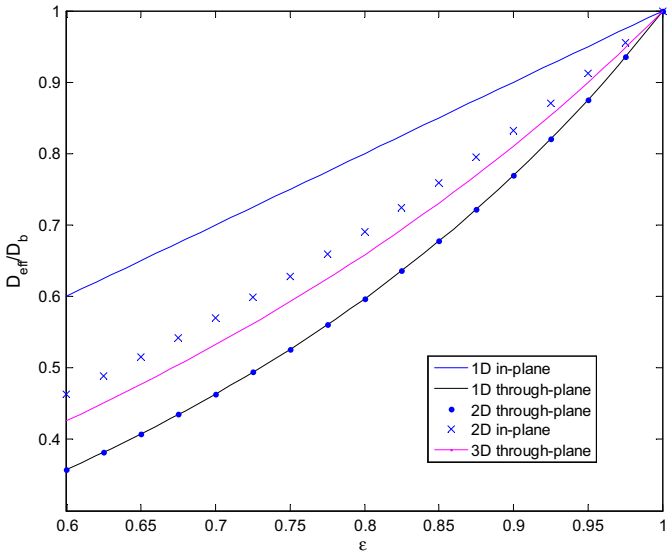

Fig. 11. Effective diffusivities for different fiber orientations.

Fig. 11 compares the effective diffusivities of randomly distributed fiber assembles with different fiber orientations. The 1D in-plane diffusivity is highest, which is easily understood as its tortuosity is unity when the fibers parallel with the diffusion direction. Both 1D fiber arrays and 2D fibrous materials normal to the diffusion direction have the highest diffusive resistance. The through-plane diffusivity of 3D fibrous material is slightly lower than the in-plane diffusivity of 2D fibrous material, both of which fall between the through-plane and in-plane diffusivities of 1D fiber arrays. In general, the effective diffusivity is enhanced with increasing fibers aligned with the diffusion direction.

4. Conclusions

Theoretical models and semi-analytical equations are proposed to predict the effective diffusivities of 1D fiber arrays, and 2D and 3D fibrous materials widely used as GDLs in PEMFCs. The predicted effective diffusivities agree well with experimentally measured values and past numerical simulation results of GDLs containing no chemical binder. Specifically, it is found that materials with randomly distributed fibers have lower diffusivities than those with fibers orderly distributed. Using less chemical binders and prevention of chemical binders filling the pores of the fibrous materials increase effective diffusivities. The present investigation is significant to the design and optimization of fibrous materials for GDLs and other applications.

Acknowledgments

The study was supported by The Hong Kong Polytechnic University Scholarship and a Discovery Project (Project ID: DP110103991) from Australia Research Council.

References

[1] J.H. Wee, Renewable and Sustainable Energy Reviews 11 (2007) 1720–1738.
[2] S. Litster, G. McLean, Journal of Power Sources 130 (2004) 61–76.
[3] W.F. Smith, J. Hashemi, Foundations of Materials Science and Engineering, McGraw-Hill Higher Education, 2006.
[4] H.L. Penman, Journal of Agricultural Science 30 (1940) 437–462.
[5] B. Bateman, J. Way, K. Larson, Separation Science and Technology 19 (1984) 21–32.

[6] P. Gibson, H. Schreuder-Gibson, D. Rivin, Colloids and Surfaces A – Physicochemical and Engineering Aspects 187 (2001) 469–481.
[7] J.H. Huang, X.M. Qian, Measurement Science & Technology 18 (2007) 3043–3047.
[8] D. Kramer, S.A. Freunberger, R. Flueckiger, I.A. Schneider, A. Wokaun, F.N. Buechi, G.G. Scherer, Journal of Electroanalytical Chemistry 612 (2008) 63–77.
[9] R. Flueckiger, S.A. Freunberger, D. Kramer, A. Wokaun, G.G. Scherer, F.N. Buechi, Electrochimica Acta 54 (2008) 551–559.
[10] M. Moest, M. Rzepka, U. Stimming, Journal of Power Sources 191 (2009) 456–464.
[11] J.M. LaManna, S.G. Kandlikar, International Journal of Hydrogen Energy 36 (2011) 5021–5029.
[12] Y.S. Chen, J.T. Fan, X. Qian, W. Zhang, Textile Research Journal 74 (2004) 742–748.
[13] J.T. Fan, Y.S. Chen, Measurement Science & Technology 13 (2002) 1115–1123.
[14] M.M. Tomadakis, S.V. Sotirchos, AICHE Journal 39 (1993) 397–412.
[15] M.M. Ahmadi, S. Mohammadi, A.N. Hayati, Physical Review E 83 (2011) 026312.
[16] E. du Plessis, S. Woudberg, J.P. du Plessis, Chemical Engineering Science 65 (2010) 2541–2551.
[17] C. Shen, G. Springer, Environmental Effect on Composite Materials, Springer, 1981.
[18] K. Ogi, N. Takeda, Journal of Composite Materials 31 (1997) 530–551.
[19] S.J. Li, L.J. Lee, J. Castro, Journal of Composite Materials 36 (2002) 1709–1724.
[20] N. Zamel, X. Li, J. Shen, Energy & Fuels 23 (2009) 6070–6078.
[21] J.H. Nam, M. Kaviany, International Journal of Heat and Mass Transfer 46 (2003) 4595–4611.
[22] J. Becker, V. Schulz, A. Wiegmann, Journal of Fuel Cell Science and Technology 5 (2008) 021006.
[23] J. Becker, C. Wieser, S. Fell, K. Steiner, International Journal of Heat and Mass Transfer 54 (2011) 1360–1368.
[24] D. Shou, J. Fan, F. Ding, International Journal of Heat and Mass Transfer 54 (2011) 4009–4018.
[25] K.J. Mattern, W.M. Deen, AICHE Journal 54 (2008) 32–41.
[26] L. Nilsson, S. Stenstrom, Chemical Engineering Science 50 (1995) 361–371.
[27] J.R. Kalnin, E.A. Kotomin, J. Maier, Journal of Physics and Chemistry of Solids 63 (2002) 449–456.
[28] V. Chen, M. Hlavacek, AICHE Journal 40 (1994) 606–612.
[29] P.N. Andrade, M.A. Fortes, Philosophical Magazine B – Physics of Condensed Matter Statistical Mechanics Electronic Optical and Magnetic Properties 58 (1988) 671–674.
[30] J.S. Ferenc, Z. Neda, Physica A – Statistical Mechanics and its Applications 385 (2007) 518–526.
[31] M.M. Tomadakis, S.V. Sotirchos, Journal of Chemical Physics 99 (1993) 9820–9827.
[32] M.A. Tahir, H.V. Tafreshi, Physics of Fluids 21 (2009) 083604.
[33] T. Stylianopoulos, A. Yeckel, J.J. Derby, X.J. Luo, M.S. Shephard, E.A. Sander, V.H. Barocas, Physics of Fluids 20 (2008) 123601.
[34] W.T. Perrins, D.R. McKenzie, R.C. McPhedran, Proceedings of the Royal Society of London Series A – Mathematical Physical and Engineering Sciences 369 (1979) 207–225.
[35] M.M.Z. Kharadly, W. Jackson, Proceedings of the Institution of Electrical Engineers – London 100 (1953) 199–212.
[36] A. Koponen, M. Kataja, J. Timonen, Physical Review E 54 (1996) 406–410.
[37] M.P. Sobera, C.R. Kleijn, Physical Review E 74 (2006) 036301.
[38] J. Becker, R. Flueckiger, M. Reum, F.N. Buechi, F. Marone, M. Stampanoni, Journal of the Electrochemical Society 156 (2009) B1175–B1181.

Nomenclature

a: edge length of square, m
C: vapor density, g m^{-3}
D_b: bulk diffusivity, m^2 s^{-1}
D_{eff}: effective diffusivity, m^2 s^{-1}
J: diffusive flux, g s^{-1} m^{-2}
l: radial distance of a cell, m
r: fiber radius, m
R: cell radius, m
S: cell area, m^2

Greek symbols
α: scale of gamma distribution
β: empirical constant
ϕ: fiber fraction
ε: porosity
ε_p: percolation threshold
θ: azimuth
Γ: gamma distribution function
τ: tortuosity